The Journal of Experimental Biology 213, 479-486

doi:10.1242/jeb.035428

Experimental study on the mechanical properties of the horn sheaths from cattle

B. W. Li, H. P. Zhao*, X. Q. Feng, W. W. Guo and S. C. Shan

AML, Department of Engineering Mechanics, Tsinghua University, Beijing 100084, China

*Author for correspondence (zhaohp@tsinghua.edu.cn)

Accepted 6 October 2009

SUMMARY

Bovine horn is composed of a sheath of keratin overlying a bony core. Previous studies of the bovine horn sheath have focused mainly on its morphology and compositions. In the present paper, we performed a series of uniaxial tension, three-point bending, and fracture tests to investigate the structural and mechanical properties of the horn sheaths from subadult cattle, *Bos taurus*. The effects of hydration on the mechanical properties were examined and their variations along the longitudinal direction of the horn sheath were addressed. Scanning electron microscopy of the fracture surfaces showed that the horn sheath has a layered structure and, more interestingly, the laminae have a rippled appearance. The Young's modulus and tensile strength increase from 850 MPa and 40 MPa at 19% water content to 2.3 GPa and 154 MPa at 0% water content, respectively. The Poisson's ratio of the horn sheath was about 0.38. The critical stress intensity factor was about 4.76 MPa m$^{1/2}$ at an intermediate hydration (8% water content), greater than that at 0% water content (3.86 MPa m$^{1/2}$) and 19% water content (2.56 MPa m$^{1/2}$). The bending properties of the samples varied along the length of the horn. The mean flexural moduli of the specimens in the distal, middle and proximal parts were about 6.26 GPa, 5.93 GPa and 4.98 GPa, respectively; whereas the mean yield strength in the distal segment was about 152.4 MPa, distinctly higher than that in the middle (135.7 MPa) and proximal parts (116.4 MPa). This study deepens our understanding of the relationships among optimal structure, property and function of cattle horn sheaths.

Key words: bovine horn, keratin, mechanical properties, biomechanics, biological materials.

INTRODUCTION

Keratin is a class of resistant and insoluble fibrous protein with the two distinct groups, namely, α- and β-keratin (Mercer, 1961). The former mainly occurs in the mammalian skins, wools, hoofs and horns, whereas the latter is the chief constituent of avian claws, scales, feathers and beaks. These keratinized tissues are usually associated with various important biological functions, e.g. offense, defense, display, communication, temperature and water regulation (Wu et al., 2004). According to the 'Ashby maps' (Ashby et al., 1995), keratin is among the toughest biological materials in nature (Wegst and Ashby, 2004). The mechanical properties of keratinous biomaterials in a broad array of taxa have been examined. Some relevant experimental results on the elastic moduli with hydration effect are summarized in Table 1, including those of hagfish thread (Fudge and Gosline, 2004), horse hoof (Bertram and Gosline, 1987; Douglas et al., 1996), donkey hoof (Collins et al., 1998), bovid hoof (Franck et al., 2006; Zhang et al., 2007), ostrich claw and feather (Bonser, 2000; Taylor et al., 2004), swan feather and goose feather (Cameron et al., 2003), human hair and nail (Baden, 1970; Wei et al., 2005), wool (Feughelman and Robinson, 1971), as well as antelope horn sheath (Kitchener and Vincent, 1987).

Similar to antelope, other bovid animals also have horns composed of a keratinous sheath overlying a bony core (Huang and Yu, 1997). Moreover, bovid horns are permanent throughout life, unlike antlers which are shed and regrown each year (Mercer, 1961). Generally, the bovid horns have evolved to function as a weapon, to inflict damage on opponents, as a shield catching the blows, and as a binding organ holding the opponent's head during pushing and wrestling contests (Geist, 1966). Hence, they are often subjected to high and repeated loads. For example, in a two-bull butting, the force on a horn can reach up to half the total weight of a bull, ~2500 N (Lofgreen et al., 1962; Phillips and Morris, 2001). In a fight between bighorn sheep the maximum force on a horn can reach about 3400 N (Kitchener, 1988). The severe deformation and failure of a horn are dangerous for bovid animals because it cannot regrow after breakage. Consequently, the horn sheath needs to have sufficiently high stiffness, strength and toughness to prevent breakage.

The composition characteristics of bovid horn sheaths have been investigated in the previous literature. The linear viscoelasticity of the horn sheath of gemsbok and the effect of water was investigated (Kitchener, 1987a). The fracture toughness of the horn sheaths of gemsbok (*Oryx gazella*), mouflon (*Ovis aries musimon*) and waterbuck (*Kobus ellipsiprymnus*) were systematically measured as a function of water and, interestingly, the results were applied to understand the horning behavior of bovids (Leuthold, 1977; Kitchener, 1987b). Furthermore, the dielectric properties of the horn sheaths of calf, cow and rhinoceros were also studied (Maeda, 1989; Marzec and Kubisz, 1997; Rizvi and Khan, 2008). The knowledge of the mechanical properties of bovid horns is helpful for gaining a deeper understanding of their natural design and adaptation of their structures and functions. However, it is somewhat surprising that there has been little attention focused on the mechanical properties of bovid horn sheaths. Pushing and wrestling contests are often observable in domestic bovine animals (Bouissou et al., 2001). Therefore, the present paper aims to investigate the microstructures and mechanical properties of the horn sheaths of domestic cattle (*Bos taurus*). Their Young's modulus, ultimate tensile strength, Poisson's ratio, flexural properties and critical stress intensity factor were systematically measured by uniaxial tension,

Table 1. Elastic moduli, *E*, of keratinous materials at three different hydration levels

Materials	Dry *E* (GPa)	Fresh *E* (GPa)	Wet *E* (GPa)	References
Oryx horn*	6.1	4.3	1.8	Kitchener and Vincent (1987)
Horse hoof (dorsal outer wall)	14.6 (0)	1.0	0.41 (100)	Douglas et al. (1996), Bertram and Gosline (1987)
Donkey hoof*	2.17	0.19	0.14	Collins et al. (1998)
Bovine hoof (dorsal wall)*	3.29	0.38	0.10	Franck et al. (2006), Zhang et al. (2007)
Ostrich claw	2.7(0)		1.84 (60) 0.14(100)	Bonser (2000), Taylor et al. (2004)
Ostrich feather	3.66 (0)		2.58 (50) 1.47(100)	Taylor et al. (2004)
Swan feather			4.11 (50)	Cameron et al. (2003)
Goose feather			4.95 (50)	Cameron et al. (2003)
Human hair†			4.8–7.5 (50)	Wei et al. (2005)
Human nail*		4.3		Baden (1970)
Wool	3.8		1.4	Feughelman and Robinson (1971)
Hagfish thread	3.6		0.006	Fudge and Gosline (2004)

*Data from bending tests. †Data from nanoindentation tests. Numbers in brackets are relative humidity in %.

three-point bending, and fracture tests. In particular, we studied the effect of hydration on the mechanical properties and their variations along the longitudinal direction of the horn. Our experiments suggest that through a long evolutionary history, the horn sheath has become adapted mechanically and functionally for effective intraspecific fighting.

MATERIALS AND METHODS

Specimen preparation

In the tests, we used six horns from three male domestic cattle (*Bos taurus* L.). Whole horns from subadult and healthy cattle of 1- to 2-years old were obtained from a local slaughterhouse (butchered for dietary reasons; Daxing District, Beijing, China). The keratin sheath was isolated naturally from the bony core. It may be divided into three segments with the same length, namely, the proximal, middle and distal segments (Fig. 1A). The thickness of the horn sheath gradually increases along its length from the proximal to the distal segment, and it is relatively uniform in the middle. We fabricated three types of test specimens along the growth axis of the horn sheath, as schematized in Fig. 1. Their geometrical dimensions, sampling directions and sampling positions were as follows. (1) The uniaxial tension specimens were taken from the middle part of the horn sheath and machined into a dumb-bell shape (Fig. 1B). (2) The three-point-bending samples were cut from the proximal, middle and distal segments in order to obtain the variations of the mechanical properties of the horn sheath along its length (Fig. 1C). (3) The specimens for fracture tests were machined from the middle part of the horn sheath. A single-edge crack was introduced in the specimen using a sharp razor blade (Fig. 1D).

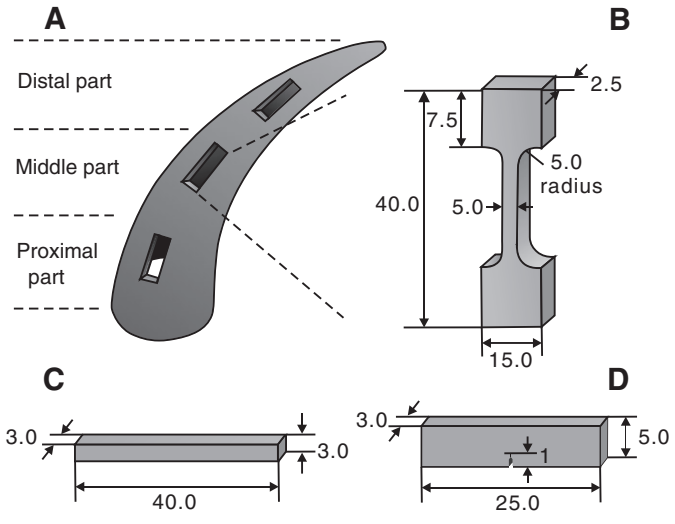

Fig. 1. Schematic drawing of a cattle horn sheath, showing the positions where the samples were cut. All the dimensions are in millimeters.

Tensile tests

Quasi-static tensile tests were conducted at room temperature using a computer-controlled universal testing machine (AG-G series, Shimadzu Corporation, Kyoto, Japan). The tests used the dumb-bell shaped samples of horn sheaths, with the dimensions of about 2.5 mm×15 mm×40 mm (thickness×width×length). Both the ends of the sample were sandwiched between two 20 mm×20 mm square aluminum grips with roughened attachment surfaces. Cyanoacrylate adhesive was used to augment the attachment. Strain gauges were mounted along the longitudinal and lateral directions on the surface of the tensile sample in order to record the axial and transverse strains. Tests were performed at a constant crosshead speed of 2 mm min^{-1} with a load cell of 2000 N. The force and displacement data were automatically recorded using a built-in measurement software.

The water content, determined by the relative decrement of the total mass upon complete drying, was used to characterize the hydration level of a sample. It ranged from 0 (completely dry) to its saturation value. To evaluate the hydration effect, the tensile samples were equilibrated at the three following water contents: (1) the samples were placed in an oven and dried at 80°C for 3 days to reach the water content of about 0%. (2) The samples were stored at ambient conditions to obtain the water content value of 8%. (3) The hydration condition of 19% water content was achieved by placing the samples in distilled water for 90 h.

To minimize the effect of variation in the experimental material, five specimens at each hydration level were measured and the results averaged.

Three-point bending tests

The flexural samples at the 8% water content were subjected to three-point bending tests at room temperature. We used a materials testing machine (Z005 series, Zwick/Roll Corporation, Ulm, Germany) with a 1000 N load cell and a crosshead speed of 2 mm min^{-1}. The dimensions of the samples were 40 mm×3 mm×3 mm (length×width×thickness). The supporting span length in tests was about 36 mm. From the three-point bending tests, one can obtain the mechanical properties of the horn sheath at different positions, from the proximal to the distal. The proximal, middle and distal segments were measured in 18, 14 and 6

specimens, respectively. The sample was continuously loaded until it ruptured on the outer surface or until the strain reached the value of 5.0%, according to ASTM standard D790-03.

Fracture tests

The parameter of critical stress intensity factor K_{IC}, which corresponds to the initiation of crack propagation, is often applied to characterize the ability of materials to resist fracture. The fracture tests on the horn sheaths were conducted to acquire the value of K_{IC} using single-edge-notched bend (SENB) specimens at room temperature with a 500 N load cell and a crosshead speed of 2 mm min^{-1}. We used the same testing machine as in the tensile tests. Each sample measured 25 mm×5 mm×3 mm (length×width×thickness) with a notch of 1 mm length in the middle. The supporting span length in tests was about 20 mm. The hydration effect on K_{IC} of cattle horn sheaths was investigated at three water content levels, as in the tensile tests. Five samples were tested under each hydration condition.

Scanning electron microscopy

The fracture surfaces of cattle horn sheaths were examined after the tensile tests. The fractured specimens were first dried at 80°C in an oven until they reached a constant mass. Then the fracture surfaces were coated with gold and observed using a scanning electron microscope (SEM: SS-550, Shimadzu Corporation, Kyoto, Japan).

Data analysis

Descriptive statistics were performed on all of the experimental data to obtain the means and the standard errors (OriginPro 7.5, OriginLab Corporation). Data are presented as the mean ± the standard error of the mean (s.e.m.). One-way analysis of variance (ANOVA) followed by Tukey's test was applied to the measured data for each experiment described above. The level of statistical significance was set at $P<0.05$.

Tensile tests

The force and displacement data obtained from each tensile test were converted to stresses and strains for analysis. We used engineering stress, defined as the ratio of the instantaneous tensile force to the initial cross-sectional area of the sample. The engineering strain is defined as the ratio between the length increment of the sample and the initial sample length. Tensile modulus E_t is a measurement of elastic stiffness for materials, calculated from the slope of the linear portion of the stress–strain curve. Ultimate tensile strength is defined as the maximum stress at the occurrence of rupture. The Poisson's ratio ν is the negative ratio between the transverse strain and the axial strain.

Three-point bending tests

Flexural modulus E_f was calculated using the following equation for three-point bending:

$$E_f = \frac{Fl^3}{48I\delta} , \quad (1)$$

where F is the applied load, l is the span length, I is the second moment of area of the flexural sample, and δ is the deflection at the loading point. The flexural modulus was calculated from the tangent of the initial slope of flexural load–displacement curve. Meanwhile, we obtain the flexural yield strength by determining the stress at which the stress–strain curve deviates by a 0.2% strain offset from the tangent to the linear elastic line (ASTM D790-03).

Fracture tests

Linear elastic fracture mechanics (LEFM) has been successfully applied to biological materials (Meyers et al., 2008; Kitchener, 1987b). The critical stress intensity factor K_{IC} of the horn sheath could be measured by standardized three-point single-edge-notched-bending (SENB) specimens (ASTM D5045-99). K_{IC} can be calculated by:

$$K_{IC} = \frac{F_c l}{BW^{3/2}} f\left(\frac{a}{W}\right) , \quad (2)$$

where F_c is the applied critical load, B and W are the thickness and width of the specimen, respectively, and a is the length of the pre-crack in the specimen. The function $f(a/W)$ is a geometry-dependent factor correlating the compliance of the specimen with the length–width ratio of the pre-crack. It is calculated by:

$$f\left(\frac{a}{W}\right) = \frac{3\left(\frac{a}{W}\right)^{\frac{1}{2}}\left[1.99 - \frac{a}{W}\left(1-\frac{a}{W}\right)\left[2.15 - 3.93\frac{a}{W} + 2.7\left(\frac{a}{W}\right)^2\right]\right]}{2\left(1+2\frac{a}{W}\right)\left(1-\frac{a}{W}\right)^{\frac{3}{2}}} . \quad (3)$$

In addition, K_{IC} can be transformed into the critical J-integral J_{IC} and the critical strain energy release rate G_{IC} by the following approximate relations:

$$J_{IC} = G_{IC} = \frac{(1-\nu^2)K_{IC}^2}{E_t} . \quad (4)$$

RESULTS

Tension

The uniaxial tension tests showed that the mechanical properties of the horn sheath are distinctly dependent on the hydration condition. The sheath is brittle at 0% water content but ductile at 8% and 19% water contents, as can be seen from the typical stress–strain curves in Fig. 2. Table 2 summarizes the mechanical properties calculated from the stress–strain curves. The mean Young's modulus of the samples at 0% water content was about 2.34±0.12 GPa, significantly greater than that at 8% water content

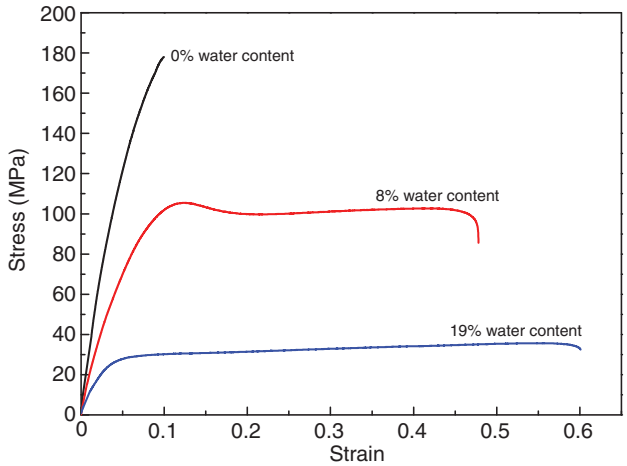

Fig. 2. Tensile stress–strain curves under three representative hydration levels.

Table 2. Tensile properties of cattle horn sheaths at three different hydration levels

Water content (%)	Young's modulus (GPa)	Tensile strength (MPa)	Tensile strain (%)	Work of fracture (MJ m^{-3})
0	2.34±0.12	154.14±11.23	11.32±1.66	12.02±2.85
8	1.56±0.06	104.53±0.84	49.30±4.46	41.63±1.69
19	0.85±0.09	39.72±2.19	56.13±4.23	19.59±0.96

Values are means±s.e.m.

(1.56±0.06 GPa) and 19% water content (0.85±0.09 GPa). The mean tensile strengths at 0%, 8% and 19% water contents were about 154.1±11.2 MPa, 104.5±0.8 MPa and 39.7±2.2 MPa, respectively. The tensile strength at 0% water content was higher than that at 8% and 19% water contents. However, the maximum tensile strain at 0% water content (11.32±1.66%) was much lower than that at 8% water content (49.30±4.46%) and 19% water content (56.13±4.23%). Consequently, the average strain energy density, also referred to as work of fracture, can be obtained from the total area under the stress–strain curve. The work of fracture at 0%, 8% and 19% water contents were calculated as 12.02±2.85 MJ m^{-3}, 41.63±1.69 MJ m^{-3} and 19.59±0.96 MJ m^{-3}, respectively. Evidently, the work of fracture at 8% water content is much higher than those at 0% and 19%. Statistical analyses indicated that the tension data of Young's modulus and tensile strength were significantly different at the three hydration levels (P<0.05). Nevertheless, there was no statistically significant difference in the ultimate tensile strains at 8% and 19% water contents (P=0.48) or in the works of fracture at 0% and 19% water contents (P=0.06). Meanwhile, from the measured transverse and axial strains of the specimens with the 8% water content, the Poisson's ratio of the fresh horn sheath was determined as 0.38±0.02.

Bending

Fig. 3 gives three typical flexural stress–strain curves of the bending specimens cut from different positions of a cattle horn sheath. Evidently, the mechanical properties vary along the length of the sheath. During the three-point bending tests, no specimen broke before the maximal tensile strain on the outer surface of the specimen reached 5%. Therefore, according to ASTM standard D790-03, the bending tests were terminated and the maximum strain was 5% for all the specimens, as shown in Fig. 3. The mean flexural moduli of the specimens in the proximal, middle and distal segments were then 4.98±0.07 GPa, 5.93±0.11 GPa and 6.26±0.12 GPa, respectively (Table 3). The mean flexural yield strength in the distal segment was about 152.4±6.9 MPa, greater than that in the middle (135.7±2.3 MPa) and the proximal segment (116.4±1.3 MPa). Statistical analyses showed a remarkable difference in the flexural yield strength in the proximal, middle and distal segments (P<0.05), whereas no significant difference was found in the flexural modulus in the middle and distal segments (P=0.13).

Table 3. Flexural properties of cattle horn sheaths at different positions along its length

Position	Flexure modulus (GPa)	Yield strength (MPa)	Number of samples
Distal part	6.26±0.12	152.4±6.9	6
Middle part	5.93±0.11	135.7±2.3	14
Proximal part	4.98±0.07	116.4±1.3	18

Values are means±s.e.m.

Fracture

Using Eqn 2 and Eqn 3, the mean critical stress intensity factor K_{IC} of the samples at 8% water content was measured to be 4.76±0.33 MPa m$^{1/2}$, considerably higher than that at 0% water content (3.86±0.19 MPa m$^{1/2}$) and 19% water content (2.56±0.21 MPa m$^{1/2}$), as shown in Fig. 4. Statistical analysis indicated no significant difference of the K_{IC} values at 0% and 8% water contents (P=0.10). With the Poisson's ratio value of 0.38, the critical strain energy release rate G_{IC} was calculated from Eqn 4 as 5.46±0.56 kJ m^{-2}, 12.55±1.77 kJ m^{-2} and 6.68±1.09 kJ m^{-2} at 0%, 8% and 19% water contents, respectively. The same values were obtained for the critical J-integral J_{IC}.

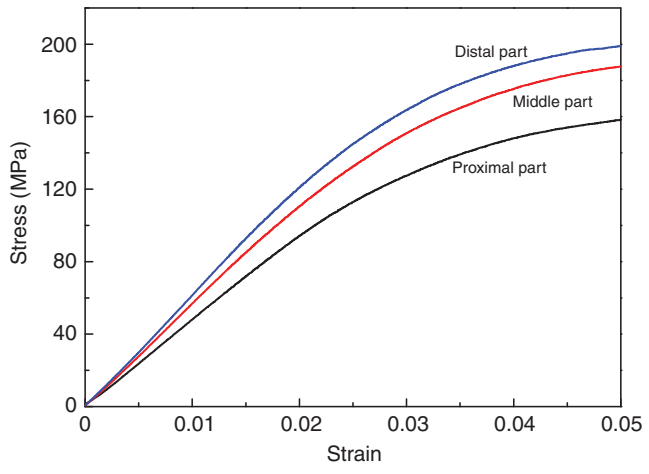

Fig. 3. Typical flexural stress–strain curves of the samples cut from different parts of the horn sheath. The bending tests were terminated when the maximum strain on the outer surface of the specimen reached 5%, according to ASTM standard D790-03.

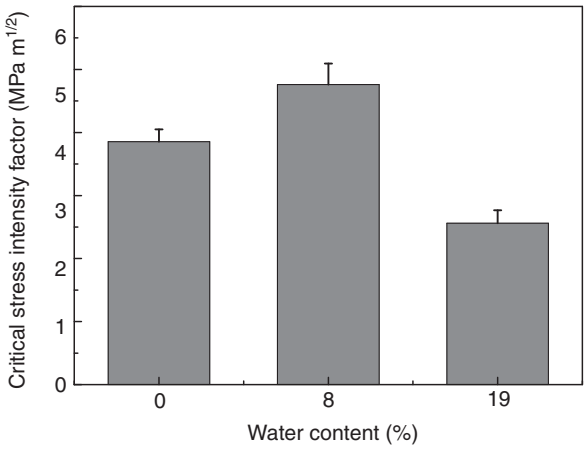

Fig. 4. Critical stress intensity factor K_{IC} of the cattle horn sheath at three different hydration levels.

Scanning electron microscopy

Scanning electron microscopy of the fracture surfaces after the tensile tests (Fig. 5A–D) clearly revealed the laminate structure of cattle horn sheath. The layered structure of the horn sheath is shown in Fig. 5A and, more interestingly, it is found that each layer has a rippled shape, consisting of a large number of flattened dead keratin-filled keratinocytes (Fig. 5B). The flattened keratinized cells have a labyrinth-like surface morphology and are laminated with each other (Fig. 5C). Jagged and tortuous crack path profiles were observed along the cell interfaces (Fig. 5B,C), leading to the stepped morphology of the fracture surfaces (Fig. 5D).

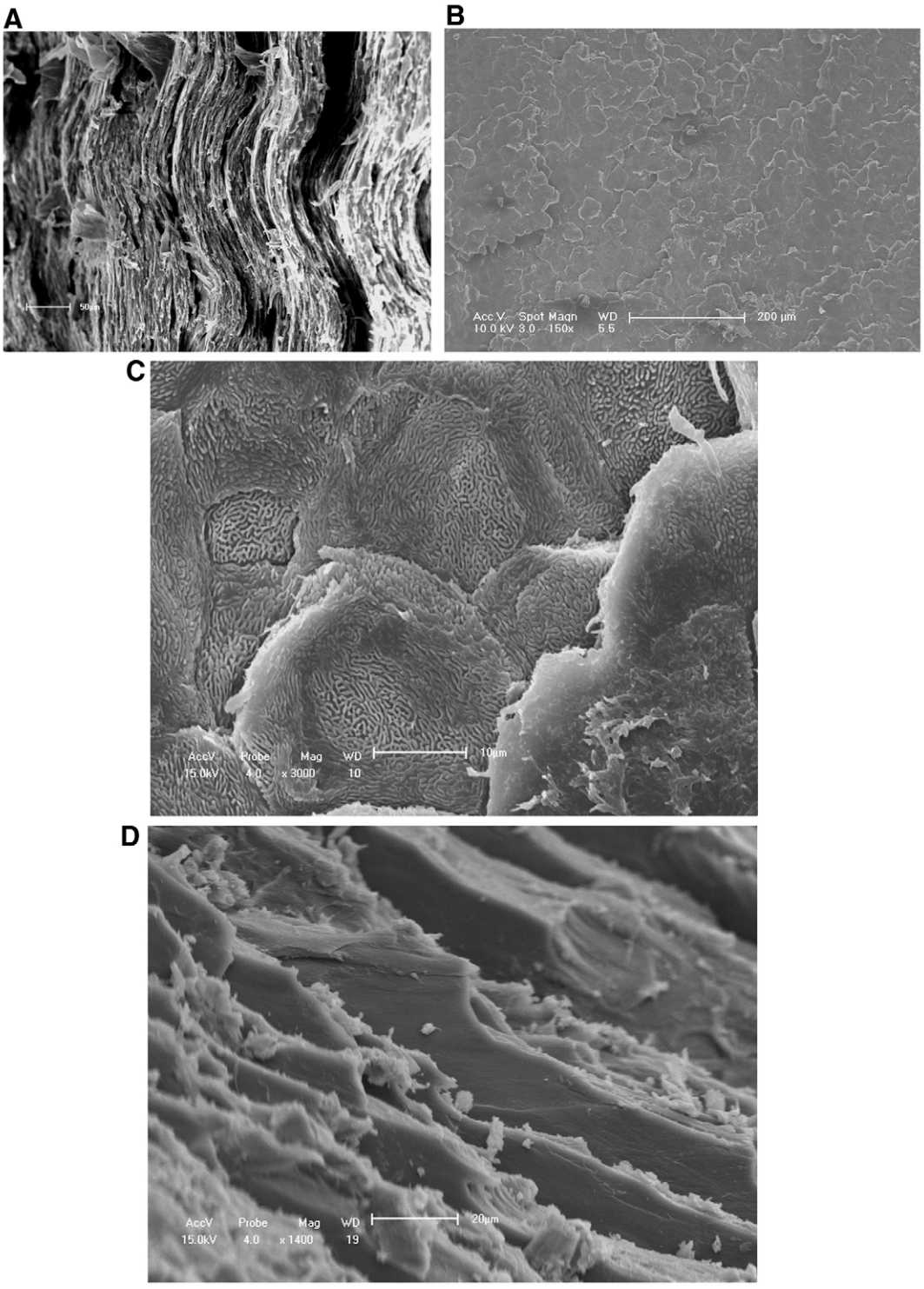

Fig. 5. Scanning electron micrographs of fracture surfaces of horn sheath specimens. (A) The layered structure of constituent tabular cells with a rippled appearance. (B) Laminated tabular cells. (C) High-magnification micrograph showing the labyrinth-like surface morphology of the lamina. (D) Stepped morphology of the fracture surface.

DISCUSSION

During combat and defense, adult cattle rely on their muscular body of more than 500 kg weight, strong horns and hooves. The big force and the high impact speed of the animal in defense can cause high stress concentrations on the horns, especially on the horn sheaths. On the one hand, the horn sheath acts effectively as a load support element to withstand large external loads without severe deformation or fracture. On the other hand, it transfers the load to the bony core along the radial direction and to the skull along the longitudinal direction. Therefore, the cattle horn sheath must have a sufficiently high stiffness and strength to prevent possible breakage, and these superior mechanical properties depend strongly on the properties of its constituent hard α-keratin material and the complicated microstructure by which the material is integrated.

Hydration dependence of mechanical properties

The mechanical properties of cattle horn sheaths, as a kind of biocomposite, depend on the mechanical parameters of the reinforcements (intermediate filaments; IFs), the matrix (keratin-associated proteins; KAPs) and their interfaces. The observed hydration sensitivity of the sheath of cattle horns is typical for many natural biological materials such as bone (Seto et al., 2008), spider silk (Gosline et al., 1999) and nacre (Barthelat and Espinosa, 2007). Similar dependence relationships have also been reported in some other keratin materials (Table 1), e.g. rhinoceros horn (Bendit and Gillespie, 1978), oryx horn (Kitchener and Vincent, 1987) and calf horn (Maeda, 1989). These experimental data demonstrate the sensitive dependence of the mechanical properties of horn keratin upon the degree of hydration. When the horn keratin is dry at 0% water content, its stiffness and strength increase but the material becomes brittle. In this case, the dry horn keratin becomes more sensitive to the presence of cracks, and it may rupture at a relatively lower strain level. When the horn keratin is overwetted with 19% water content, the material becomes too weak to resist high loads, while the material has the largest work of fracture at 8% water content. Previous studies on the horn sheaths of gemsbok, mouflon and waterbuck also found maximum toughness when it was in the fresh state (Kitchener, 1987b). Furthermore, the sensitive dependence of the horn properties upon the hydration degree was also applied to infer the horning behavior of bovids. With the horning behavior, bovid animals dipped their horns into mud or plants to avoid the dehydration of the horn keratin and to ensure its adapted mechanical properties (Kitchener, 1987b).

Furthermore, α-keratin materials have different forms in nature, varying from the filamentous type of hair and wool to the laminations of cattle horn. The specific form of α-keratin is thought to be mainly determined by the network of hydrogen-bonds (Kitchener and Vincent, 1987), covalent disulphide bonds (Hearle, 2000) and intermolecular cross-links such as ionic interactions and van der Waals bonds (Fraser et al., 1986; Parry, 1996; Kreplak and Fudge, 2007). Previous experimental studies found a progressive increase of water mobility and a decrease in structural rigidity of α-keratin with hydration (Speakman, 1928; King, 1945). From the viewpoint of molecular interactions, water may weaken the hydrogen-bond network by disassociating some intermolecular cross-links and, therefore, reduce the effective bonding in the α-keratin materials (Kitchener and Vincent, 1987). For such reasons, a higher hydration in α-keratin materials will lead to a lower yield stress (Hearle, 2000). From the viewpoint of polymer composites, the influence of hydration on the properties of the matrix phase is more significant than that on the denser microfibrillar phase (Bertram and Gosline, 1987). Owing to the relative lack of secondary bonding, the matrix phase often exhibits a lower stiffness and a higher extensibility than the fibrous phase. In addition, a modified Voigt model has been used to estimate the stiffness of oryx horns in terms of the shear modulus of the matrix and the effective length of the fibers in response to hydration (Kitchener and Vincent, 1987).

Variations of mechanical properties along the horn length

The results of our three-point bending tests revealed a spatially varying feature in such flexural properties as flexural modulus and yield strength of the cattle horn sheaths. It can be easily understood that in order to efficiently bear the applied force without severe deformation or rupture, the cattle horn should possess higher flexural modulus, strength and fracture toughness at the thinner end. During defense, the slender proximal part has the function of stabbing the opponent, thus it needs higher strength and stiffness, whereas the proximal part should be more flexible to absorb energy in wrestling. The gradient variations of the stiffness and strength in a horn sheath are attributed to different water contents and keratinization degrees in the proximal, middle and distal parts. In other words, the spatially variations of the mechanical property of the horn sheath depend mainly upon the mechanical function, environment, materials and microstructures. In addition, the flexural modulus measured in the tests is distinctly higher than the tensile modulus. The reasons are as follows. Firstly, the wavy layered structure and the rough interfaces between neighboring layers in the horn sheath may contribute to the higher flexural modulus (Farran et al., 2009). Moreover, the keratin horn sheath possesses a relatively lower modulus under tension than that under compression, as has been reported for horse hoof (Douglas et al., 1996). This flexural property is in accord with the fact that the horn mainly suffers bending instead of uniaxial tension. Similar result was also found in other keratinous materials. For example, adult human fingernail was documented to have the flexural modulus of 4.0–5.0 GPa, much higher than its tensile modulus of about 2.0–3.0 GPa (Baden, 1970; Farran et al., 2009).

Fracture behavior

A crack or scratch may form on the horn sheath surface during fighting. Therefore, it is of interest to consider the fracture behavior of the horn sheath for understanding its functional reliability. Importantly, it was found that the horn sheath exhibits very high fracture resistance, which is critical for maintaining its biological functions. Its mean K_{IC} varies from 2.56 MPa m$^{1/2}$ at 19% water content to 4.76 MPa m$^{1/2}$ at 8% water content. Somewhat surprisingly, the K_{IC} of the horn sheath is of the same order as that of bone (2–5 MPa m$^{1/2}$) (Nalla et al., 2003) and abalone sheath (8±3 MPa m$^{1/2}$) (Sarikaya et al., 1990), and it exceeds those of the enamel and dentin in teeth (0.7–1.3 MPa m$^{1/2}$, 1–2 MPa m$^{1/2}$, respectively) (Nalla et al., 2003). Moreover, the maximum work of fracture of the cattle horn sheath is obtained at a water content of 8% (fresh), as is consistent with the maximum K_{IC} value at the same hydration level. According to Eqn 4, the value of G_{IC} in fresh cattle horn keratin is about 12.55 kJ m^{-2}, significantly larger than that of the fresh mouflon horn, about 8.4 kJ m^{-2} (Kitchener, 1987b). However, the calculated G_{IC} at 19% water content is about 6.68 kJ m^{-2}, lower than that of fully hydrated horse hoof (12.0 kJ m^{-2}) (Bertram and Gosline, 1986), and bovine hoof at 100% RH of (8.48 kJ m^{-2}) (Clark and Petrie, 2007). In addition, the way the test specimens are notched has a certain amount of influence on the measured G_{IC} (Tattersall and Tappin, 1966). In the study, the widely adopted single-edge-notched bend (SENB) specimens were used to determine the K_{IC} values.

Microstructure and toughening mechanisms

The microstructures of cattle horn sheaths are distinctly different from those of other hard α-keratins of mammalian appendages. The equine hoof horn has a tubular structure with tubules of about 200 μm in diameter (Kasapi and Gosline, 1999). The white rhinoceros horn has a similar tubule microstructure, composed of cortex, medullary cavity and intertubular matrixes (Hieronymus et al., 2006). Antler is highly mineralized, with a structure similar to bone (Kierdorf et al., 2000). Wool and human hair fibers have a hierarchical fibrous structure (Hearle, 2000; Popescu and Hocker, 2007). In this study, we observed that the cattle horn sheath keratin has a laminar structure consisting of flattened, curved dead keratin-filled epithelial cells (Fig. 5), which is somewhat similar to that of the mouflon horn sheath (Kitchener, 1987b) and toucan beak keratin (Seki et al., 2005).

This microstructure of cattle horn sheath leads to an enhanced toughening effect on the fracture resistance. Firstly, the wavy interface between the flattened cells may effectively resist the nucleation and propagation of cracks. A crack can propagate only along a tortuous or branching path, rendering a higher dissipation of fracture energy. Similar toughening mechanisms have also been observed in some other natural laminar materials, such as nacre (Jackson et al., 1988; Sarikaya et al., 1990), sponge spicules (Levi et al., 1989; Sarikaya et al., 2001; Aizenberg et al., 2005) and giant clam shells (Lin et al., 2006). Moreover, the labyrinth-like surface on the flatted cell may enhance the friction between the lamina in the horn sheath and thus restrain the relative movement of neighboring lamina. Meanwhile, the lamina structure may help maintain an appropriate hydration level, which may be essential for optimum toughness of the material. Further experimental and theoretical investigations will be of great interest in gaining an insight of the toughening mechanisms of cattle horn sheath.

In conclusion, we have studied the microstructure and mechanical properties of cattle horn sheath keratin from the domestic cattle. Knowledge of the mechanical properties of cattle horn sheaths is essential for understanding the optimal design and adaptation of their structures and functions. The present results may also be relevant to the keratin horn sheath of the wild cattle, a rare and endangered animal. Finally, it is worth mentioning that more experiments are needed to further investigate the dependence of the mechanical properties of the horn sheaths on such factors as age, sex, temperature, degree of keratinization and water absorption.

ACKNOWLEDGEMENTS

The support of the National Natural Science Foundation of China (Grants No. 10872116, 10732050 and 10525210) and 973 program of MOST (2010CB631005) are acknowledged.

REFERENCES

Aizenberg, J., Weaver, J. C., Thanawala, M. S., Sundar, V. C., Morse, D. E. and Fratzl, P. (2005). Skeleton of *Euplectella* sp.: Structural hierarchy from the nanoscale to the macroscale. *Science* **309**, 275-278.

Ashby, M. F., Gibson, L. J., Wegst, U. and Olive, R. (1995). The mechanical properties of natural materials. I. Material property charts. *Proc. R. Soc. Lond. A* **450**, 123-140.

Baden, H. P. (1970). The physical properties of nail. *J. Invest. Dermatol.* **55**, 115-122.

Barthelat, F. and Espinosa, H. D. (2007). An experimental investigation of deformation and fracture of nacre-mother of pearl. *Exp. Mech.* **47**, 311-324.

Bendit, E. G. and Gillespie, J. M. (1978). The probable role and location of high-glycine-tyrosine proteins in the structure of keratins. *Biopolymers* **17**, 2742-2745.

Bertram, J. E. and Gosline, J. M. (1986). Fracture toughness design in horse hoof keratin. *J. Exp. Biol.* **125**, 29-47.

Bertram, J. E. and Gosline, J. M. (1987). Functional design of horse hoof keratin: the modulation of mechanical properties through hydration effects. *J. Exp. Biol.* **130**, 121-136.

Bonser, R. H. C. (2000). The Young's modulus of ostrich claw keratin. *J. Mater. Sci. Lett.* **19**, 1039-1040.

Bouissou, M. F., Boissy, A., Neindre, P. L. and Veissier, I. (2001). The social behaviour of cattle. In *Social Behavior in Farm Animals* (ed. L. J. Keeling and H. W. Gonyou), pp.113-146. Wallingford, Oxon: CABI Publishing.

Cameron, G. J., Wess, T. J. and Bonser, R. H. C. (2003). Young's modulus varies with differential orientation of keratin in feathers. *J. Struct. Biol.* **143**, 118-123.

Clark, C. and Petrie, L. (2007). Fracture toughness of bovine claw horn from cattle with and without vertical fissures. *Vet. J.* **173**, 541-547.

Collins, S. N., Cope, B. C., Hopegood, L., Latham, R. J., Linford, R. G. and Reilly, J. D. (1998). Stiffness as a function of moisture content in natural materials: Characterisation of hoof horn samples. *J. Mater. Sci.* **33**, 5185-5191.

Douglas, J. E., Mittal, C., Thomason, J. J. and Jofriet, J. C. (1996). The modulus of elasticity of equine hoof wall: implications for the mechanical function of the hoof. *J. Exp. Biol.* **199**, 1829-1836.

Farran, L., Ennos, A. R., Starkie, M. and Eichhorn, S. J. (2009). Tensile and shear properties of fingernails as a function of a changing humidity environment. *J. Biomech.* **42**, 1230-1235.

Feughelman, M. and Robinson, M. S. (1971). Some mechanical properties of wool fibers in the "Hookean" region from zero to 100% relative humidity. *Text. Res. J.* **41**, 469-474.

Franck, A., Cocquyt, G., Simoens, P. and De Belie, N. (2006). Biomechanical properties of bovine claw horn. *Biosyst. Eng.* **93**, 459-467.

Fraser, R. D., MacRae, T. P., Parry, D. A. and Suzuki, E. (1986). Intermediate filaments in α-keratins. *Proc. Natl. Acad. Sci. USA* **83**, 1179-1183.

Fudge, D. S. and Gosline, J. M. (2004). Molecular design of the α-keratin composite: insights from a matrix-free model, hagfish slime threads. *Proc. R. Soc. Lond. B* **271**, 291-299.

Geist, V. (1966). The evolution of horn-like organs. *Behaviour* **27**, 175-214.

Gosline, J. M., Guerette, P. A., Ortlepp, C. S. and Savage, K. N. (1999). The mechanical design of spider silks: from fibroin sequence to mechanical function. *J. Exp. Biol.* **202**, 3295-3303.

Hearle, J. W. S. (2000). A critical review of the structural mechanics of wool and hair fibres. *Int. J. Biol. Macromol.* **27**, 123-138.

Hieronymus, T. L., Witmer, L. M. and Ridgely, R. C. (2006). Structure of white rhinoceros (*Ceratotherium simum*) horn investigated by X-ray computed tomography and histology with implications for growth and external form. *J. Morphol.* **267**, 1172-1176.

Huang, T. L. and Yu, P. (1997). Analysis of α-keratins in the horns of rhinoceros and buffalo by non-native capillary isoelectric focusing. *Chromatographia* **46**, 437-439.

Jackson, A. P., Vincent, J. F. V. and Turner, R. M. (1988). The mechanical design of nacre. *Proc. R. Soc. Lond. B* **234**, 415-440.

Kasapi, M. A. and Gosline, J. M. (1999). Micromechanics of the equine hoof wall: optimizing crack control and material stiffness through modulation of the properties of keratin. *J. Exp. Biol.* **202**, 377-391.

Kierdorf, U., Kierdorf, H. and Boyde, A. (2000). Structure and mineralisation density of antler and pedicle bone in red deer (*Cervus elaphus* L.) exposed to different levels of environmental fluoride: a quantitative backscattered electron imaging study. *J. Anat.* **196**, 71-83.

King, G. (1945). Permeability of keratin membranes to water vapour. *T. Faraday. Soc.* **41**, 479-487.

Kitchener, A. (1987a). Effect of water on the linear viscoelasticity of horn sheath keratin. *J. Mater. Sci. Lett.* **6**, 321-322.

Kitchener, A. (1987b). Fracture toughness of horns and a reinterpretation of the horning behavior of bovids. *J. Zool.* **213**, 621-639.

Kitchener, A. (1988). An analysis of the forces of fighting of the blackbuck (*Antilope cervicapra*) and the bighorn sheep (*Ovis canadensis*) and the mechanical design of the horn of bovids. *J. Zool.* **214**, 1-20.

Kitchener, A. and Vincent, J. F. V. (1987). Composite theory and the effect of water on the stiffness of horn keratin. *J. Mater. Sci.* **22**, 1385-1389.

Kreplak, L. and Fudge, D. (2007). Biomechanical properties of intermediate filaments: from tissues to single filaments and back. *BioEssays* **29**, 26-35.

Leuthold, W. (1977). Agonistic behavior. In *African Ungulates: A Comparative Review of Their Ethology and Behavioral Ecology*, pp. 109-138. Berlin: Springer-Verlag.

Levi, C., Barton, J. L., Guillemet, C., Le Bras, E. and Lehuede, P. (1989). A remarkably strong natural glassy rod: the anchoring spicule of the *Monorhaphis* sponge. *J. Mater. Sci. Lett.* **8**, 337-339.

Lin, A. Y. M., Meyers, M. A. and Vecchio, K. S. (2006). Mechanical properties and structure of *Strombus gigas*, *Tridacna gigas*, and *Haliotis rufescens* sea shells: A comparative study. *Mater. Sci. Eng. C* **26**, 1380-1389.

Lofgreen, G. P., Hull, J. L. and Otagaki, K. K. (1962). Estimation of empty body weight of beef cattle. *J. Anim. Sci.* **21**, 20-24.

Maeda, H. (1989). Water in keratin. Piezoelectric, dielectric, and elastic experiments. *Biophys. J.* **56**, 861-868.

Marzec, E. and Kubisz, L. (1997). Dielectric relaxation of air-dried horn keratin. *Int. J. Biol. Macromol.* **20**, 161-165.

Mercer, E. H. (1961). The keratinized tissues. In *Keratin and Keratinization: An Essay in Molecular Biology* (ed. P. Alexander and Z. M. Bacq), pp. 64-66. New York: Pergamon Press.

Meyers, M. A., Chen, P. Y., Lin, A. Y. M. and Seki, Y. (2008). Biological materials: Structure and mechanical properties. *Prog. Mater. Sci.* **53**, 1-206.

Nalla, R. K., Kinney, J. H. and Ritchie, R. O. (2003). Effect of orientation on the in vitro fracture toughness of dentin: the role of toughening mechanisms. *Biomaterials* **24**, 3955-3968.

Parry, D. A. D. (1996). Hard α-keratin intermediate filaments: an alternative interpretation of the low-angle equatorial X-ray diffraction pattern, and the axial disposition of putative disulphide bonds in the intra- and inter-protofilamentous networks. *Int. J. Biol. Macromol.* **19**, 45-50.

Phillips, C. J. C. and Morris, I. D. (2001). The locomotion of dairy cows on floor surfaces with different frictional properties. *J. Dairy Sci.* **84**, 623-628.

Popescu, C. and Hocker, H. (2007). Hair-the most sophisticated biological composite material. *Chem. Soc. Rev.* **36**, 1282-1291.

Rizvi, T. Z. and Khan, M. A. (2008). Temperature-dependent dielectric properties of slightly hydrated horn keratin. *Int. J. Biol. Macromol.* **42**, 292-297.
Sarikaya, M., Gunnison, K. E., Yasrebi, M. and Aksay, J. A. (1990). Mechanical property – microstructural relationships in abalone shell. In *Materials Synthesis Utilizing Biological Processes*, vol. 174, pp. 109-166. Pittsburgh, Pennsylvania: Mater. Res. Soc.
Sarikaya, M., Fong, H., Sunderland, N., Flinn, B. D., Mayer, G., Mescher, A. and Gaino, E. (2001). Biomimetic model of a sponge-spicular optical fiber – mechanical properties and structure. *J. Mater. Res.* **16**, 1420-1428.
Seki, Y., Schneider, M. S. and Meyers, M. A. (2005). Structure and mechanical behavior of a toucan beak. *Acta. Mater.* **53**, 5281-5296.
Seto, J., Gupta, H. S., Zaslansky, P., Wagner, H. D. and Fratzl, P. (2008). Tough lessons from bone: Extreme mechanical anisotropy at the mesoscale. *Adv. Funct. Mater.* **18**, 1905-1911.
Speakman, J. B. (1928). The plasticity of wool. *Proc. R. Soc. Lond. B* **103**, 377-396.
Tattersall, H. G. and Tappin, G. (1966). The work of fracture and its measurement in metals, ceramics and other materials. *J. Mater. Sci.* **1**, 296-301.
Taylor, A. M., Bonser, R. H. C. and Farrent, J. W. (2004). The influence of hydration on the tensile and compressive properties of avian keratinous tissues. *J. Mater. Sci.* **39**, 939-942.
Wegst, U. G. K. and Ashby, M. F. (2004). The mechanical efficiency of natural materials. *Philos. Mag.* **84**, 2167-2181.
Wei, G. H., Bhushan, B. and Torgerson, P. M. (2005). Nanomechanical characterization of human hair using nanoindentation and SEM. *Ultramicroscopy* **105**, 248-266.
Wu, P., Hou, L. H., Plikus, M., Hughes, M., Scehnet, J., Suksaweang, S., Widelitz, R. B., Jiang, T. X. and Chuong, C. M. (2004). Evo-Devo of amniote integuments and appendages. *Int. J. Dev. Biol.* **48**, 249-270.
Zhang, D. S., Arola, D. D., Reprogel, R. K., Zheng, W., Tasch, U. and Dyer, R. M. (2007). A method for characterizing the mechanical behaviour of hoof horn. *J. Mater. Sci.* **42**, 1108-1115.